

AperTO - Archivio Istituzionale Open Access dell'Università di Torino

Toward a novel framework for bloodstains dating by Raman spectroscopy: How to avoid sample photodamage and subsampling errors

This is a pre print version of the following article:

Original Citation:

Availability:

This version is available <http://hdl.handle.net/2318/1721723> since 2025-01-17T11:55:43Z

Published version:

DOI:10.1016/j.talanta.2019.120565

Terms of use:

Open Access

Anyone can freely access the full text of works made available as "Open Access". Works made available under a Creative Commons license can be used according to the terms and conditions of said license. Use of all other works requires consent of the right holder (author or publisher) if not exempted from copyright protection by the applicable law.

(Article begins on next page)

Toward a novel framework for bloodstains dating by Raman spectroscopy: how to avoid sample photodamage and subsampling errors

Alicja Menzyk^{1*}, Alessandro Damin², Agnieszka Martyna¹, Eugenio Alladio^{2,3}, Marco Vincenti^{2,3}, Gianmario Martra², Grzegorz Zadora^{1,4}

¹ Institute of Chemistry, University of Silesia in Katowice, Szkolna 9, 40-007 Katowice, Poland

² Department of Chemistry, University of Torino, Via P. Giuria 7, 10125 Torino, Italy

³ Centro Regionale Antidoping e di Tossicologia "A. Bertinaria", Regione Gonzole 10/1, 10043 Orbassano, Torino, Italy

⁴ Institute of Forensic Research, Westerplatte 9, 31-033 Krakow, Poland

ABSTRACT: Answers to questions about the time of bloodstains formation are often essential to unravel the sequence of events behind criminal acts. This study provided a Raman-based procedure, designated for probing into the chemistry of ageing bloodstains. To circumvent limitations experienced with single-point measurements – the risk of laser-induced degradation of hemoglobin and subsampling errors – the rotating mode of spectral acquisition was introduced. In order to verify the performance of this novel sampling method, obtained spectra were confronted with those acquired during conventional static measurements. The visual comparison was followed by analysis of data structure using regularized MANOVA, which boosted the variance between differently-aged samples while minimizing the variance observed for bloodstains deposited at the same time. Studies of relation between these variances demonstrated the superiority of novel procedure, as it provided Raman signatures that enabled a better distinction between differently-aged bloodstains.

A blood trace deposited at a crime scene, a real treasure trove for forensic experts, is often considered as the main driving force beyond the development of criminal investigations. This is because properly handled blood-related evidentiary material can establish a strong link between an individual and a criminal act or even allow for the reconstruction of bloodshed events, owing to the methods of bloodstain pattern analysis. As a consequence, the wealth of the investigative information, gained by the examination of blood traces, quite often can lead to a major U-turn in a course of forensic proceedings. In certain cases, however, this blood-derived body of data can point the trier of fact in an entirely wrong direction, unless the information about the time of trace formation is provided.

The value of this time-related data and its contribution to criminal investigations are easily comprehensible. Situating preserved evidence to the case at hand or even help in the chronological reconstruction of past events. Unfortunately, confrontation with the issue of time is probably one of the most challenging tasks ever faced by the forensic community¹. Hence, despite relentless efforts to solve the problem, a reliable method for estimating the time elapsed since bloodstain deposition (or time since deposition, TSD) still remains beyond the reach of forensic science. As it was reported in^{2,3}, all of already conducted studies have confirmed the time-dependent behaviour of physicochemical properties of blood deposits. Nevertheless, none of developed methods has exhibited the precision and reproducibility regarded as a *conditio*

sine qua non of their successful implementation in standard forensic proceedings.

The answer to the question of bloodstains' age, as with all forensic dating tasks, may be considered achievable owing to changes of blood properties that take place during the evidence degradation. Once the bloodstain is created, its initial composition becomes more diverse due to the cascade of physicochemical processes, which involve mainly hemoglobin (Hb) – the dominant component of dried blood traces^{2,3}. Redistribution of electrons within π heme's orbitals, as well as changes of the heme pocket geometry that take place during the formation of Hb degradation products (see Figure S1), trigger conformational rearrangements in polypeptide chains. These subtle structural distortions are reflected in physicochemical properties of bloodstains, which quite easily can be probed with suitable analytical tools^{2,3}, and subsequently linked to the passage of time.

To date, the vast majority of methods developed for estimating the absolute age of the trace have been guided by one simple principle – they have sought the above-mentioned dependency between the TSD and some dynamic bloodstains properties. In most cases, this task has been completed through the employment of regression analysis, where an equation relating measured values of ageing parameter (i.e. ageing markers) and the absolute age of bloodstains is established^{2,3}. However, this approach might be not entirely correct. After all, equations underlying these calibration models, intended for predicting the TSD of questioned materials, always modelled the ageing behaviour of samples that were degrading

Eliminato: Development of an improved Raman-based procedure using sample rotation

Eliminato: Gianmario Martra²,

Formattato: Italiano (Italia)

Eliminato: Unfortunately, the relevance of preserved evidence to the committed offence usually cannot be verified, because forensic experts are still incapable of providing an accurate estimate of the bloodstains' age. An antidote to this impediment might be substituting the classical dating approach – founded on the application of calibration models – by the comparison problem addressed using likelihood ratio tests. The key aspect of this concept involves comparing the evidential data with results characterizing reference bloodstains, formed during the process of supervised ageing so as to reproduce the evidence. Since this comparison requires data that conveys information inherent to changes accompanying the process of blood decomposition, t

Eliminato: intends to

Eliminato: (B)

Eliminato: (W)

Eliminato: B and W

Formattato: Tipo di carattere: Grassetto

Eliminato: – s

Eliminato: ,

Eliminato: hence

Eliminato: ; however

under tightly-controlled laboratory conditions. And that is what remains the main reason for delayed exploitation of already developed dating methods in routine caseworks. It goes without saying that the crime scene reality hardly ever resembles laboratory settings. The vicissitudes of environment and blood biology mean that no two degradation pathways are exactly alike. Thus, using dating models trained on the reference datasets might lead to misestimations of TSD, depriving these models of almost entire practical value.

It does not mean, however, that, because of these difficulties, questions regarding the time aspect of bloodstains formation should be withdrawn from the courtroom scenario. It just means that these queries should be tackled in a different manner, and exactly this endeavor – the quest for the novel framework for bloodstains dating – constitutes the backbone of the presented research. It is hypothesized that impediments resulting from the variability of ageing kinetics could be addressed by substituting a case-suited comparison problem, considered for example within a likelihood ratio (LR) methodology⁷, for the conventional dating approach. The key aspect of this concept is to estimate the (dis)similarity between the stage of evidence degradation and sets of reference materials, obtained through the process of supervised ageing, simulating – as closely as possible – the actual settings of evidence decomposition at the crime scene (Figure S2). Obviously, in order to enable this comparison, information inherent to changes accompanying the process of blood degradation still have to be delivered, therefore the aim of this study was to provide the first component of the aforementioned novel dating approach by developing a Raman-based analytical method, serving as a tool for characterizing the state of bloodstains degradation.

The choice of Raman spectroscopy (RS) is coherent with its maturation as a powerful technique in the analysis of biosamples⁵, especially heme-containing proteins⁶. It has been revealed that the vast majority of bands comprising Raman spectra of Hb, isolated erythrocytes and even whole blood originate from vibrational modes involving the C–C, C=C, and C–N bonds of the porphyrin ring within the heme structure⁶⁻⁸, which are highly sensitive to even minute structural changes of the protein. Thus, this particular feature of hemoproteins vibrational spectra holds promise for adapting RS to bloodstains dating studies, as it should give an insight into formation of different Hb derivatives over time. And indeed, the time-dependent behaviour of Raman spectra of blood deposits has been already demonstrated⁹⁻¹¹. However, despite this valuable discovery, there are still some challenges that continually hamper implementation of Raman-based methodology in standard proceedings. One of these obstacles might be representative probing of the chemical composition of degrading bloodstains, which is usually pursued through acquisition of a few single-point measurements within different areas of the sample⁹⁻¹¹. However, dried deposits of body fluids are not only physically, but also chemically heterogeneous, hence this sampling mode might result in poor reproducibility of measurements and, in the long term, misestimations of TSD.

In view of the above, this study intended to expand the current Raman-based approaches largely through eradication of the risk of the laser-induced degradation of bloodstains^{3,9,12} and subsampling errors. In order to do so, the rotating measurement mode that involved spinning the bloodstain sample during the spectral acquisition by means of a magnetic-driven

sample-holder^{13,14} was established, and subsequently employed for characterizing the behaviour of bloodstains during three-week degradation period. To verify the capability of the novel sampling method to provide data that facilitated discerning differently-aged blood traces, its performance was compared with the routinely applied single-point sampling procedure (the static mode).

EXPERIMENTAL SECTION

Sample preparation

All experiments were conducted on blood drawn from a single donor in order to mitigate the possible influence of inter-individual factors on the variability of spectral responses. 20 μL aliquots of capillary blood, obtained by finger puncture, were transferred (without the addition of preservatives) into aluminum sample pans – yielding almost featureless background that did not interfere with Raman scattering – and then allowed to dry for two hours before spectrum collection.

During the entire study, two classes of bloodstains were employed. The first class, which was used for conducting experiments for selecting the setup of spectral acquisition, comprised four groups of six bloodstains. Each of these groups served for testing different levels of laser power (for details see *Raman instrumentation and sample presentation*). Regarding the second class, namely the population of samples used for ageing studies, two separate sets consisting of six bloodstains each, respectively for rotating and static measurement modes, were created. Deposited bloodstains were then stored, protected from any light sources, for three weeks under **conditioned** laboratory conditions (temperature: 23.6 ± 2.0 °C, relative humidity: $30 \pm 4\%$).

All the blood samples were deposited at time intervals so as to compensate the different duration of spectral acquisition in the static and rotating modes, and through that equalize the ongoing transformations of bloodstains, which are particularly rapid at the initial stage of ageing^{2,3}.

Raman instrumentation and sample presentation

The spectra were recorded in the range $300\text{--}1800$ cm^{-1} using a Renishaw inVia Raman Microscope spectrometer, equipped with a $5\times$ objective and a 785-nm laser line. Due to the exceptional susceptibility of Hb to laser irradiation^{3,9,12}, the rotating measurement mode – aimed at reducing the excitation-induced damages – was introduced, and confronted with the conventional single-point measurements. In order to indicate parameters allowing for non-invasive spectral acquisition, the ratio between the band at 1227 cm^{-1} and one of the previously identified Hb aggregation marker^{3,12} – a spectral feature at 1248 cm^{-1} – was monitored for four groups of bloodstains, created independently for the static and rotating measurements. Each of these groups were analyzed with increasing power of the excitation source – 0.5%, 1%, 5% and 10% of its maximum value (~ 103 mW on the sample) to verify whether upon increasing the power, any of the monitored ratios significantly decreased, which would be indicative of laser-induced detrimental effects. Throughout this power test, the exposure time and number of accumulations were adapted separately for each excitation power, so as to maintain the comparable number of counts, and thereby provide Raman spectra of similar signal-to-noise ratio.

Monitoring the progress of bloodstains degradation

Eliminato: , hence

Subsequently, in order to investigate the time-dependent behaviour of bloodstains, samples were analyzed every two hours (from two up to eight hours elapsed since bloodstain formation) and then once per day for the period of three weeks. All of Raman spectra were registered concomitantly in both measurement modes.

Data pre-processing

Right at the beginning, the original spectra were truncated to omit the range 300–600 cm^{-1} , which was severely affected by the noise and increasing baseline. As a result, each spectrum covered the range 600–1800 cm^{-1} , which included most of Raman bands associated with the vibrational modes of target analytes (Hb and its derivatives).

Subsequently, in order to mitigate the effect of fluorescence, an adaptive iteratively reweighted penalized least squares (airPLS) fitting procedure, introduced by Zhang et al.¹⁵ was applied. In this technique no user intervention (e.g. band detection) is required, and the baseline itself is gradually approximated by weighted penalized least squares method. Weighting is provided to the sum of squared differences between the original spectrum and the estimated baseline to eliminate the bands and focus only on baseline points during the approximation procedure. Since the performance of this correction method might be negatively affected by noise factors, a third-order Savitzky-Golay filter was applied prior to background subtraction – using 21-point and 17-point windows in case of the static and rotating modes, respectively – and was followed by the logarithmic transformation and mean-centering, aimed at ensuring the homogeneity of data variance.

Finally, in order to alleviate unwanted inter-spectra distortions, and through that reveal genuine temporal behaviour of Raman features, the background-corrected Raman spectra were subjected to the probabilistic quotient normalization (PQN)¹⁶. During this procedure, the normalization factor for each spectrum was indicated as a median of quotients, which were obtained by dividing the acquired spectrum by a reference (the median signal).

It should be also clearly stated that the choice of the pre-processing strategy was based on the thorough visual inspection of corrected signals. However, the problem of optimizing the spectral pre-processing can be automated, for example by using genetic algorithms¹⁷, which is the subject of our further work.

Comparison between the performance of the static and rotating sampling modes using rMANOVA

The prerequisite for any effective discrimination is that the average variance of the replicate measurements within each group is much lower than the variance of groups averages. If this condition is not satisfied, distributions of variables characterizing the compared groups will overlap, preventing from successful discrimination. That also applies to LR models⁴ designed for distinguishing between differently-aged bloodstains.

Among methods of variance analysis offered by the contemporary chemometrics, there are several tools suited for studying highly correlated multivariate data sets. One of them is a regularized multivariate analysis of variance (rMANOVA), which – unlike its prototype (MANOVA) – is suitable for data populations containing more variables than samples¹⁸. The main goal of this method is defining new directions (eigenvec-

tors) that boost the between-group variance, (denoted as **B**), whilst minimizing the within-group variance, (denoted as **W**).

In this study, a single group comprised Raman spectra of bloodstains characterized by the same TSD values, hence the variation within measurements of equally-aged bloodstains corresponded to within-group variance **W**; whilst the between-group variance **B**, equaled to the variation of the averages of bloodstains deposited at different times. In order to evaluate the capability of both measurement modes to provide data that facilitate discrimination of bloodstains in terms of their TSD, and, through that, to verify which of those two methods (static or rotating) should be implemented in future LR-based dating procedure, rMANOVA was employed to compare the variance structure of registered Raman spectra. Taking into account that in the case of univariate data, all matrices are substituted by scalars, e.g. **B** becomes b^2 , the b^2 to w^2 ratio was investigated on the first eigenvector (first canonical variate, CV1), being the direction maximizing the b^2/w^2 Q .

Additionally, static and rotating datasets comprising spectra registered over whole degradation period (three weeks) were divided into three subgroups, corresponding to spectra acquired within the first seven, 14 and 21 days of degradation. For each of these subgroups the b^2/w^2 were calculated, so as to investigate the changes of the performance of both modes with progression of time.

All the mathematical background of the research was carried out using the R software (version 3.3.1)¹⁹.

RESULTS AND DISCUSSION

Optimization of a Raman spectra acquisition setup

The motivation for choosing the 785-nm excitation was threefold. First of all, owing to the previous studies of Lemler et al.⁹ and the group of Sato²⁰, it has been demonstrated that the Raman spectrum of whole blood acquired with 785 nm laser line, does not provide information about any other of its constituents but our target analytes – Hb protein and its derivatives. Secondly, exploiting the laser wavelength distant from the electronic absorption region of fluorescent components of blood allowed to avoid overlapping the photoluminescence phenomenon with the informative Raman scattering. And finally, it was also crucial to ensure that the process of spectral acquisition did not alter the Hb, which is known for its susceptibility to photodegradation^{9,12,21}. The exploitation of excitation source outside the range of electronic transitions of Hb derivatives, which include weak Q-band (α and β) between 490–650 nm and the most intense Soret band in the region of 400–436 nm²³, allowed to reduce the risk of the increased absorption of the electromagnetic radiation, with consequent heating of the sample, triggering formation of undesirable laser-induced heme aggregation products^{12,21}.

The above-mentioned precaution against forced degradation of bloodstains might not be sufficient, because the photo-induced denaturation can appear within the nominally non-resonant region of Hb, even if using laser irradiation of relatively low power.^{9,12} An example of such an undesired effect is depicted in Figure 1a, which illustrates spectral symptoms attributed to the laser-triggered degradation that occurred while performing measurements of the static sample with 785 nm excitation. The sudden change of spectral features can be clearly observed for spectra of static bloodstains registered with 10% of initial laser power and with 5%, however to a much lower level. The Raman

Eliminato: W

Commentato [G1]: Concomitantly? How it was possible?

Eliminato: (denoted as

Eliminato:)

Eliminato: (denoted as

Eliminato:)

Eliminato: T

Eliminato: in the case of univariate data, all matrices are substituted by scalars, e.g. **B** becomes b^2

Eliminato: Over the last few years, application of near-IR radiation for Raman examinations of body fluids has been gaining rapid interest for a variety of reasons. In case of this study, the

Eliminato:

Eliminato: which might have resulted in the local

Eliminato: (call it briefly $B \gg W$)

Eliminato:)

Eliminato: Unfortunately, t

Eliminato: . This is

Eliminato: , as already evidenced in the literature^{9,12},

Eliminato: whose effectiveness can be linked with $W^{-1}B$ values characterizing the multivariate data.

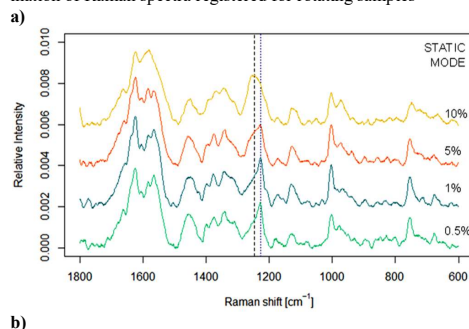
Eliminato: Apart from an enhancement of fluorescence intensity (not indicated in the figure), t

signature of photodegraded bloodstain consists of broader spectral features in comparison to those registered with lower levels of laser power (0.5% and 1%). In addition, changes in the relative intensity of several component occurred, and the signal at 1248 cm⁻¹ – deserves particular attention, as it served herein as a marker of laser-induced degradation, while deciding on non-invasive parameters of spectral acquisition.

The choice of this degradation indicator was also based on the chemistry underlying its occurrence. In the recent studies of Lednev's group^{10,11} this spectral feature was assigned to the frequency of amide III band (characteristic of random coil conformation), whilst Wood et al.^{22,23} suggested that the whole spectral range between 1200 and 1300 cm⁻¹, and thus also the 1248 cm⁻¹ aggregation marker, should be interpreted as the signatures of the C_m-H methine vibrations within protoporphyrin IX moiety of heme (for labeling scheme of iron protoporphyrin IX see Figure S3). Both suggested assignments are reasonable explanations of observed laser-induced alterations, since each of these vibrations might be affected by heme stacking and protein interactions that take place during the process of blood photodegradation.

Having looked at spectra in Figure 1a it becomes clear that if one aims at obtaining good-quality Raman signatures while avoiding the photodamage of Hb, high power coupled with short acquisitions should be substituted by low excitation power combined with long acquisition times. Precisely for this reason, application of conventional static mode, when monitoring the time-dependent behaviour of heterogeneous materials, might pose some technical difficulties. And that is because providing a representative Raman signature, which in case of single-point measurements can be only obtained by performing multiple measurements across the sample, is hardly possible within short space of time.

Fortunately, the problem of laser power and interconnected time resolution can be mitigated by a relatively simple solution applied in this study – implementation of rotating measurement mode^{13,14}. Since in this case the irradiated point of the bloodstain is being constantly refreshed, the excitation energy is distributed over a larger area, hence the risk of sample damaging can be significantly reduced. Noteworthy, the visual examination of Raman spectra registered for rotating samples



b)

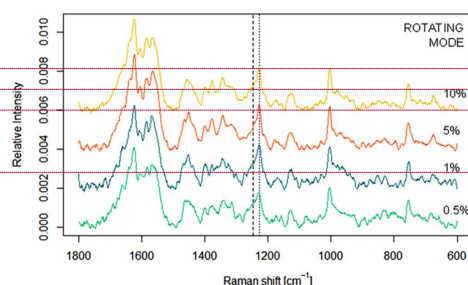


Figure 1. Influence of the laser power on Raman spectra of 2-hour bloodstains registered with 785 nm excitation laser in the (a) static and (b) rotating mode. The ratio between intensities of heme aggregation marker at 1248 cm⁻¹ (dashed line) and a stable band at 1227 cm⁻¹ (dotted line) served as an indicator of Hb photodegradation while deciding on non-invasive measurement parameters. Spectra were treated according to the procedure set forth in *Data pre-processing* and shifted for better visualization.

(Figure 1b) revealed that even the signals acquired with 10% of initial laser power were deprived of spectral features typical of decomposed bloodstains. The difference in the trends qualitatively determined by direct inspection of set of data as those in the panels of Figures 1 were fully confirmed by calculating the ratio between the band at 1227 cm⁻¹ and the aforementioned modification marker at 1248 cm⁻¹ for all sets of measurements. The results are presented in the form of ratios distribution (boxplots) in Figure S4. Therefore eventually, the signal acquisition in the static mode was performed using ten 20-s accumulations with 1% and in the rotating mode – two 20-s accumulations with 10% of initial excitation laser power – since both of these setups allowed to reduce to a minimum duration of spectral acquisition, whilst mitigating the detrimental influence of the laser.

Visual inspection of time-dependency of Raman spectra

Having established the procedures of static and rotating sampling methods, the study entered the next phase, which was solely devoted to monitoring the ageing behaviour of blood traces. The most prominent time-dependent trend, readily observed among registered signals, was an increase of baseline intensity, which might be attributed to the enhancement of bloodstains fluorescence (Figure S5a, S5c). Unfortunately, the root cause of this phenomena as yet has not been fully explained. Among numerous blood constituents, endogenous fluorophores can be identified, an example of which are aromatic amino acids, dihydronicotinamide-adenine dinucleotide phosphate (NADPH) or flavin adenine dinucleotide (FAD). However, laser wavelength exploited in this study (785 nm) was distant from the electronic absorption regions of these components, hence they could not have been the origin of observed fluorescence. Likewise Hb, or more precisely heme embedded within its structure, also should be excluded from considerations. Admittedly, porphyrins and among them a precursor of heme – protoporphyrin IX – exhibit fluorescence when excited in the NIR range, however this emission is significantly quenched when the tetrapyrrole ring is bound to iron ions³. Consequently, fresh whole blood does not exhibit NIR autofluorescence²⁴, in contrast to degraded bloodstains⁹⁻¹¹.

Eliminato: as the excitation power increases, several new bands appear

Eliminato: one of them –

Eliminato: corresponding to

Eliminato: Apart from the evident power-dependent behaviour of 1248 cm⁻¹ band, t

Eliminato: And even though the origin of 1248 cm⁻¹ band is still debatable, b

Commentato [GM5]: Please, add “1248” and “1227” labels aside relevant lines, in the panels

Eliminato: should be preferred over

Eliminato: high power coupled with short acquisitions.

Eliminato: With the aim of verifying these observations and thereby choosing optimal measurement parameters – allowing for fast and non-invasive analysis of bloodstains – the

Eliminato: aggregation

Eliminato: was monitored

Eliminato: both static and rotating measurement modes. Results of this comparison, which has been presented

Eliminato: proved initial conclusions based on the visual examination of Raman spectra (Figure 1

Eliminato: While in case of the rotating mode no damaging effects have been observed at each level of laser power, in case of the static measurements

Eliminato: bloodstains irradiated with 10% and 5% of excitation power were degraded more significantly (these findings were subsequently confirmed using one-way ANOVA test).

Eliminato: And indeed

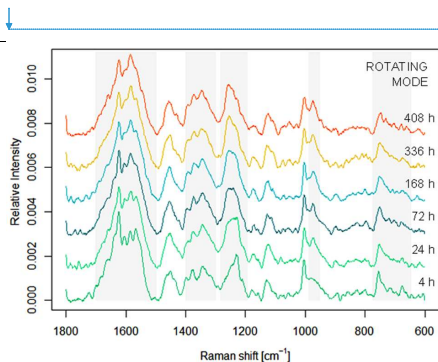


Figure 2. Exemplary Raman signatures of ageing bloodstains registered with 785 nm excitation laser in the rotating mode (an equivalent of this plot corresponding to the static mode can be found in Figure S6). Time-dependent bands are indicated in grey. Spectra were treated according to the procedure set forth in *Data pre-processing* and shifted for better visualization.

Nevertheless, inferring about bloodstains TSD solely from the fluorescence signal, increasingly dominating the Raman

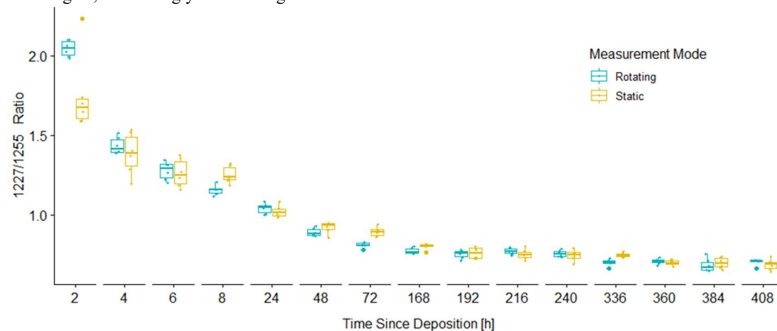


Figure 3. Boxplots representing intensity ratios of Raman bands at 1227 cm⁻¹ and 1255 cm⁻¹ against the age of static and rotating bloodstains (given in hours).

Nevertheless, ambiguities concerning the root causes of those bands should not diminish the usefulness of Raman spectroscopy in dating studies. By plotting the time behaviour of ratios of bands at 1227 cm⁻¹ and 1255 cm⁻¹ (Figure 3), called later 1227/1255 ratio, it can be clearly observed that rapid decrease of their value within first few days of degradation would allow to distinguish between differently-aged bloodstains. This differentiation would be more effective in case of rotating mode, as no overlap between distributions of ratios corresponding to *different (???)* time-points was observed contrary to static bloodstains (*see, for instance, pairs of data at 4 and 6 hours, and at 6 and 8 hours*) which was the initial evidence of superior reproducibility of spectra obtained using the novel sampling mode.

Variance analysis with rMANOVA – comparison between the static and rotating mode

scatter, is rather risky, simply because variation in the baseline may also derive from factors other than formation of degradation products (e.g. changing sampling geometry). Therefore, prior to further data analysis, spectra were baseline corrected to expose changes within Raman bands, which co-evolved with the fluorescence enhancement. The effects of this correction procedure are presented in Figure S5.

A pictorial view of the background-corrected Raman signals (Figure 2) revealed subtle, but noticeable alterations appearing in bands pattern as a function of time. Once again our attention was drawn to changes occurring in the range of 1220–1300 cm⁻¹, which bore a strong resemblance to laser-induced spectral distortions (compare with Figure 1). A distinctive and relatively sharp band at about 1227 cm⁻¹ was broadening with progression of time, moving through maximum reached at ca. 1248 cm⁻¹ to end up forming a band at 1255 cm⁻¹. As already discussed in *Optimization of a Raman spectra acquisition setup*, the origin of this temporal behaviour has long evaded the understanding of scientists, who attributed it either to conformational changes of protein^{10,11} or alterations of C_m-H methine vibrations within heme moiety^{22,23}.

Notwithstanding the evident time-dependent behaviour of the monitored 1227/1255 ratio, its adoption in dating task has some obvious limitations. First of all, the manual rating of the bloodstains' age through this particular spectral feature is not applicable at long time scales, as the ratio values level off rather quickly – in case of this study after c.a. 168 h (seven days) of natural degradation (Figure 3). Besides, inferring the TSD from the changes of 1227/1255 ratio limits dating capabilities of the method, as it considers information encoded in a single spectral feature, while ignoring the interactive effects of other potentially-informative dynamic-variables.

In order to indicate any other time-changes in registered Raman spectra, and through that verify whether further distinction between similarly-aged bloodstains would be achievable, the inspection of b²/w² values corresponding to each value of Raman shift was performed (Figure 4). A listing of these time-dependent spectral features, characterized by values of b²/w² above unity, was gathered in Table S1. As it can be seen,

Eliminato: As evidenced also in case of this study, the fluorescence enhancement of blood deposits was constantly progressing over time, hence the most probable origin of this phenomenon was accumulation of degradation products. Owing to the previous studies^{24–28}, it was established that decomposed Hb exhibits fluorescent properties, resulting possibly from the dissociation of Hb subunits followed by the release of iron ions. In order to complete the picture, it should be also added that electron spin resonance studies of bloodstains had previously revealed signal, allegedly originating from non-heme iron, which was increasing with degradation time²⁹. In light of the above, it is hard to escape the impression that this degradation pathway would somehow resemble the *in vivo* blood recycling process

Eliminato: ,

Eliminato: However, in our opinion, another possible explanation of this phenomenon should be also considered. Given the presumptive conclusions about formation of heme-breakdown products based on the trend of increasing fluorescence, one could presume that the pattern of bands within 1220–1300 cm⁻¹ is characteristic of these decomposition products. Interestingly, recent studies of Yan et al.²⁶ and Neugebauer et al.²⁷ demonstrated presence of similar spectral features in case of Raman spectra of heme metabolites (although measured in solutions). Due to the resonance effect upon

Eliminato: excitation with NIR laser (λ_{ex}=752 nm), enhancement of bands at 1253 cm⁻¹ and 1243 cm⁻¹ was observed, which were subsequently identified as marker bands for bilirubin and biliverdin, respectively²⁶. In case of bilirubin, the marker band (1253 cm⁻¹) was assigned to CH-, NH-, and OH-bending vibrations; whilst the spectral feature of biliverdin (1243 cm⁻¹) to CH, NH, and OH-bending vibrations. Therefore, the presence of similar bands in our spectra of degraded bloodstains (Figure 2), combined with disappearance of feature at 1227 cm⁻¹ – δ(C_mH) – and increasing intensity of 974 cm⁻¹ band – assigned to methine bridge deformation³⁰ – might indeed suggest, but by no means prove, the breakdown of the heme moiety and emergence of some forms of open-chain tetrapyrroles. Taken together one thing is certain: an in-depth examination of bloodstains *ex vivo* decomposition is still required, as all evidence suggests that heme- and hemochromes might be not the only degradation products of blood traces.

Commentato [GM7]: Please, add *1255, 1227, 974 labels to relevant signals

Eliminato: where metHb is metabolized to globin chains and heme, followed by the enzymatic conversion of the latter to biliverdin and bilirubin^{24,26,27,30}. Due to this heme breakdown, iron is released, hence Hb metabolites show significant fluorescence. As yet, however, it has been neither confirmed, nor denied if this type of decomposition can proceed *ex vivo*, because the issue of whether heme degradation is solely enzymatic or also non-enzymatic remains unresolved^{29,31}.

Eliminato: 192

Eliminato: eight

Eliminato: the same

b^2/w^2 values close zero were obtained are present in positions typical of bands attributable to non-heme related Hb constituents – such as amide I (1655 cm^{-1}) or CH_2/CH_3 amino acid deformation modes (1450 cm^{-1}), indicating that this structural motifs of Hb remained rather stable in time. For the rest, apart from the broadly discussed $1220\text{--}1300\text{ cm}^{-1}$ region, the variation between spectra of differently-aged bloodstains appeared to be primarily due to changes observed at higher Raman shifts – ranges of $1650\text{--}1500\text{ cm}^{-1}$ and $1400\text{--}1300\text{ cm}^{-1}$ – which are known to contain so-called core-size and oxidation markers of Hb⁸, respectively. The crucial piece of information here is that these changes in characteristics of Hb are well-recognized effects of the formation of its degradation products^{9–12}.

Having demonstrated that Raman spectra of ageing bloodstains provide a wealth of chemical information, hidden within hundreds spectral features other than $1227/1255$ ratio, the discrimination capabilities of both measurement modes were examined in depth using rMANOVA, which took into account correlation among these variables. In agreement with data in Figure 3, the calculated b^2/w^2 along CV1 demonstrated that the rotating mode of spectral acquisition was indisputably better than the conventional procedure in terms of its potential discriminating capabilities, because higher values of ratios were obtained (see Figure 5). Indeed, the movement of the sample allowed to provide, at given time-point, truly averaged spectral characteristics of chemically heterogeneous bloodstain, which was reflected in low rates of w^2 ,

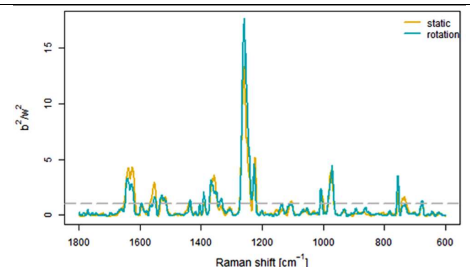


Figure 4. The b^2/w^2 values corresponding to each value of Raman shift. Grey dashed line indicates $b^2=w^2$.

characterizing dispersion of measurements of the blood samples with the same TSD.

As time progressed and degradation ceased, the gradual decline in b^2/w^2 values was noted. In addition, differences between ratios obtained for static and rotating modes were diminishing, because the distributions of degradation products along the surface of bloodstains were getting more and more uniform. Nevertheless, the superiority of rotating mode in terms of superior discriminating capability for period as long as three weeks clearly appeared. This heralds successful implementation of newly developed Raman-based procedure in the LR-based comparison approach for estimating time elapsed since bloodstains deposition.

CONCLUSIONS

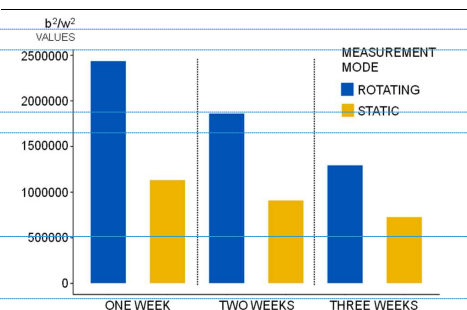


Figure 5. Comparison of b^2/w^2 values (on the first eigenvector, CV1) characterizing data sets obtained in rotating and static mode after one, two and three weeks of bloodstains degradation.

The comparison of signals registered in the rotating mode with those acquired for static bloodstains demonstrated that the former sampling method should be preferred over the conventional measurements for two reasons. First of all, as regards the reproducibility of obtained spectral signatures, the rotating mode allowed to reduce the risk of subsampling errors. This point was objectively confirmed by the analysis of data using rMANOVA, which revealed that, in case of rotating mode, the variance between Raman spectra registered for bloodstains deposited at the same time (w^2) was significantly lower than the variance observed between spectral signatures of differently-aged blood traces (b^2). It means that the novel sampling method contributed to exposing the genuine time-related changes in the Raman spectra whilst reducing the variability resulting from the inhomogeneity of the probed sample, and thereby facilitated the discrimination of bloodstains varying in TSD. This level of representativeness simply could not have been achieved through the performance of repeated static measurements in different areas of the sample. Especially, if the analysis should be carried out in the shortest possible time, as is the case with monitoring the initial stage of ageing process. Which brings us to the second reason behind advocating for the rotating mode, namely the duration of measurements. Since the application of the spinning device allowed to constantly renew the irradiated area of bloodstains, the laser-induced damaging of the specimen could have been decreased to a negligible extent. This, in turn, made it possible to register the Raman spectra using higher laser power, leading to the reduction in the length of measurements, down to XX minutes????? in comparison to the conventional static approach, lasting YY minutes?????

However, even though the conducted study allowed to place the rotating mode of Raman spectroscopy among front-line analytical tools capable of providing chemical insight into the time-dependent behaviour of bloodstains, it cannot be denied that there is more to evidence dating than simply collecting data. As with all forensic tasks, an elastic dating approach that takes into account all the factors influencing the validity of the evidence evaluation is the key to success. Unfortunately, no two crime scenes are ever exactly the same, as is often the ageing kinetics of blood traces. Precisely for this reason, establishing a universal framework for TSD estimations may be cumbersome, if not impossible to accomplish. So, despite

Formattato: Non Apice / Pedice

Eliminato: most of these bands originated from vibrational modes of the heme structure, while

Eliminato: –

Eliminato: A

Commentato [GM9]: Does'nt matter to summarise here the content of the quoted paper

Eliminato: The first group of mentioned Raman bands gives an insight into porphyrin distortions that accompany changes of the central porphyrin-core size and the spin state of iron ion, the second is sensitized to alterations in the electron density in the π heme's orbitals⁸.

Eliminato: Therefore, if b^2/w^2 patterns could have been correlated to specific Raman bands attributed to Hb derivatives, it means that Raman spectroscopy is indeed an adequate analytical tool for characterizing the state of bloodstains degradation.

Commentato [GM13]: Why values on the Y axis are of the order of $10^2\text{--}10^6$, whereas in Figure 4 they reach ca 20, at maximum? There was some cumulation?

Commentato [GM14]: On the X axis the time period should be reported in hours, for the sake of comparison with data in Figure 3. The best should be something as: 168 h (1 week), etc.

Eliminato: led to the implementation of procedure involving spinning the sample while spectral acquisition.

Eliminato: C

Eliminato: As expected after the visual inspection of

Eliminato: This observation, however, should not come as a surprise. After all

Eliminato: Furthermore, the differences between the groups of bloodstains varying in TSD were most pronounced on the scale of the first week, when the ongoing degradation changes were escalating. For both modes, during the very first few days of ageing, the highest b^2/w^2 values were observed. However, owing to more effective reduction of within-group variability in case of the novel sampling mode, ratios corresponding to rotating measurements were almost twice as high as those characterizing the static dataset. Therefore, especially in the initial stage of the ageing, when the conventional single-point measurements are particularly vulnerable to subsampling errors, employment of rotating mode should be the most beneficial.

Commentato [GM15]: The average duration in the two cases must be reported

Eliminato: However, despite the decrease of degradation rate, it was demonstrated that discerning differently-aged bloodstains would be still possible ($b^2 > w^2$), and, what is even more important, the superiority of rotating mode in terms of this discriminating capability was clearly demonstrated within the entire degradation period (Figure 5). That, in turn,

Eliminato: Errors may appear at every level of evidence evaluation starting with sampling and ending with interpretation of obtained results. Therefore, it is essential to ensure high quality of each examination phase. This study targeted the initial stage of the bloodstains dating procedure by pursuing a Raman-based method capable of representative probing the chemical composition of degrading blood traces. A method, which subsequently could be embedded in the novel methodology of

Eliminato: the evidence dating, founded on the concept of super-vised ageing.¶ The urgency of providing the representative spectrum from large area of degrading bloodstains over a short period of time,

technological advances, the question remains – how to incorporate the uncertainty deriving from the influence of factors affecting the ageing processes into the dating approach? It appears virtually impossible, but also somehow unreasonable to develop in advance dating models for each possible scenario that could be encountered at a hypothetical crime scene, hence the solution should be sought elsewhere, perhaps by looking at the dating problem from an entirely different perspective. Our future studies will be therefore primarily focused on reframing the issue of evidence dating by substituting the LR-based comparison procedure for conventional calibration models, which eventually may re-shape our notion of what is achievable in terms of the evidence dating.

ASSOCIATED CONTENT

Supporting Information

The Supporting Information is available free of charge on the ACS Publications website.

Simplified pathway of *ex vivo* hemoglobin degradation; Outline of the LR-based approach for estimating TSD of bloodstains; Scheme of iron protoporphyrin IX labelling; Distribution of intensity ratios between peaks located at 1227 cm^{-1} and 1248 cm^{-1} serving as a degradation marker during power tests; Effect of pre-processing of Raman spectra; Exemplary Raman signatures of ageing bloodstains registered in the static mode; Table containing positions and local coordinates of time-dependent Raman bands.

AUTHOR INFORMATION

Corresponding Author

*E-mail: alicja.menzysk@gmail.com

Author Contributions

The manuscript was written through contributions of all authors.

Notes

The authors declare no competing financial interest.

REFERENCES

- (1) Weyerhann, C.; Ribaux, O. Situating forensic traces in time. *Sci. Justice* 2012, 52, 68–75.
- (2) Bremmer R.H., de Bruin K.G., van Gemert M.J.C., van Leeuwen T.G., Aalders M.C.G., Forensic quest for age determination of bloodstains, *Forensic Sci. Int.* 2012, 216, 1–11.
- (3) Zadora G., Menzyk A., In the pursuit of the holy grail of forensic science e Spectroscopic studies on the estimation of time since deposition of bloodstains, *TrAC* 2018, 105, 137–165.
- (4) Zadora G., Martyna A., Ramos D., Aitken C., *Statistical Analysis in Forensic Science: Evidential Value of Multivariate Physicochemical Data*, Wiley, Chichester, 2014.
- (5) Butler H. J., Ashton L., Bird B., Cinque G., Curtis K., Dorney J., Esmonde-White K., Fullwood N.J., Gardner B., Martin-Hirsch P.L., Walsh M.J., McAinsh M.R., Stone N., Martin F.L., Using Raman spectroscopy to characterize biological materials, *Nat. Protoc.* 2016, 11, 664–687.
- (6) Atkins C.G., Buckley K., Blades M.W., Turner R.F.B., Raman spectroscopy of blood and blood components, *Appl. Spectrosc.* 2017, 71, 767–793.
- (7) Hu S.Z., Smith K.M., Spiro T.G., Assignment of protoheme resonance Raman spectrum by heme labeling in myoglobin, *J. Am. Chem. Soc.* 1996, 118, 12638–12646.
- (8) Rousseau D. L., Ondrias M. R., Raman scattering, in: D. L. Rousseau (Ed.) *Optical Techniques in Biological Research*, Academic press, inc., Orlando, 1984, pp. 100–108.
- (9) Lemler P., Premasiri W.R., DelMonaco A., Ziegler L.D., NIR, Raman spectra of whole human blood: effects of laser-induced and *in vitro* hemoglobin denaturation, *Anal. Bioanal. Chem.* 2014, 406, 193–200.
- (10) Doty K.C., McLaughlin G., Lednev I.K., A Raman “spectroscopic clock” for bloodstain age determination: the first week after deposition, *Anal. Bioanal. Chem.* 2016, 408, 3993–4001.
- (11) Doty K.C., Muro C.K., Lednev I.K., Predicting the time of the crime: bloodstain aging estimation for up to two years, *Forensic Chem.* 2017, 5, 1–47.
- (12) Dasgupta R., Ahlawat S., Verma R. S., Uppal A., Gupta P. K., Hemoglobin degradation in human erythrocytes with long-duration near-infrared laser exposure in Raman optical tweezers, *J. Biomed. Opt.* 2010, 15, 055009.
- (13) Signorile M., Bonino F., Damin A., Bordiga S., A novel Raman setup based on magnetic-driven rotation of sample, *Top. Catal.* 2018, 61, 1491–1498.
- (14) A. Damin et al. (2017) European Patent No. WO2017077513 (A1).
- (15) Zhang Z.-M., Chen S., Liang Y.-Z., Baseline correction using adaptive iteratively reweighted penalized least squares, *Analyst* 2010, 135, 1138–1146.
- (16) Dieterle F., Ross A., Schlotterbeck G., Senn H., Probabilistic Quotient Normalization as robust method to account for dilution of complex biological mixtures. Application in 1H NMR metabolomics, *Anal. Chem.* 2006, 78, 4281–4290.
- (17) Goldberg D.E., *Genetic Algorithms in Search, Optimization and Machine Learning*, Addison-Wesley, Berkeley, 1989.
- (18) Engel J., Blanchet L., Bloemen B., Heuvel L., Engelke U., Wevers R., Buydens L., Regularized MANOVA (rMANOVA) in untargeted metabolomics, *Anal. Chim. Acta* 2015, 89, 1–12.
- (19) R. Core Team. R: A Language and Environment for Statistical Computing. R Foundation for Statistical Computing, Vienna, Austria, 2012 ISBN 3-900051-07-0. <http://www.R-project.org/>.
- (20) H. Sato, H. Chiba, H. Tashiro, Y.J. Ozaki, Excitation wavelength-dependent changes in Raman spectra of whole blood and hemoglobin: comparison of the spectra with 514.5, 720, and 1064 nm excitation, *Biomed. Opt.* 6 (2001) 366–370.
- (21) Ramser K., Bjerneld E.J., Fant C., Käll M., Importance of substrate and photoinduced effects in Raman spectroscopy of single functional erythrocytes, *J. Biomed. Opt.* 2003, 8, 173–178.
- (22) Wood B.R., Hammer L., Davis L., McNaughton D., Raman microspectroscopy and imaging provides insights into heme aggregation and denaturation within human erythrocytes, *J. Biomed. Opt.* 2005, 10, 14005–14013.
- (23) Wood B.R., Caspers P., Puppels G.J., Pandiancherri S., McNaughton D., Resonance Raman spectroscopy of red blood cells using near-infrared laser excitation, *Anal. Bioanal. Chem.* 2007, 387, 1691–1703.
- (24) Htun N.M., Chen Y.C., Lim B., Schiller T., Maghzal G.J., Huang A.L., Elgass K.D., Rivera J., Schneider H.G., Wood B.R., Stocker R., Peter K., Near-infrared autofluorescence induced by intraplaque hemorrhage and heme degradation as marker for high-risk atherosclerotic plaques, *Nat. Commun.* 2017, 8, 1–16.
- (25) Panter S.S., Release of iron from hemoglobin, *Methods Enzymol.* 1994, 231, 502–514.
- (26) Yan D., Domes C., Domes R., Frosch T., Popp J., Pletz M.W., Frosch T., Fiber enhanced Raman spectroscopic analysis as a novel method for diagnosis and monitoring of diseases related to hyperbilirubinemia and hyperbiliverdinemia, *Analyst* 2016, 141, 6104–6115.
- (27) Neugebauer U., März A., Henkel T., Schmitt M., Popp J., Spectroscopic detection and quantification of heme and heme degradation products, *Anal. Bioanal. Chem.* 2012, 404, 2819–2829.
- (28) Nagababu E., Rifkind J.M., Heme Degradation during Autoxidation of Oxyhemoglobin, *Biochem. Biophys. Res. Commun.* 2000, 273, 839–845.

(29) Miki T., Kai A., Ikeya M., Electron spin resonance of bloodstains and its application to the estimation of time after bleeding, *Forensic Sci. Int.* 1987, 35, 149–158.

(30) Celis F., Campos-Vallette M.M., Gómez-Jeria J.S., Clavijo R.E., Jara G.P., Garrido C., Surface-enhanced Raman scattering and

theoretical study of the bilichromes biliverdin and bilirubin, *Spectrosc. Lett.* 2016, 49, 336–342.

(31) Schaefer W.H., Harris T.M., Guengerich F.P., Characterization of the Enzymatic and Nonenzymatic Peroxidative Degradation of Iron Porphyrins and Cytochrome P-450 Heme, *Biochemistry* 1985, 24, 3254–3263.

Table of contents only:

